



# A model-data integrated iterative learning controller for flexible tracking with application to a piezo nanopositioner

Transactions of the Institute of  
Measurement and Control  
2018, Vol. 40(10) 3201–3210  
© The Author(s) 2018  
Reprints and permissions:  
sagepub.co.uk/journalsPermissions.nav  
DOI: 10.1177/0142331217719958  
journals.sagepub.com/home/tim



Zhao Feng, Jie Ling, Min Ming and Xiaohui Xiao

## Abstract

In precise motion systems, feedforward controller is a key component for significant performance enhancement. However, traditional iterative learning control (ILC) works efficiently under strictly repetitive reference input, and the performance of model-based feedforward controllers is limited by the non-minimum phase zeros and modeling uncertainties during executing tasks. In this paper, a model-data integrated ILC is proposed for flexible tracking, where the stable part of the identified model is utilized to compose the model-based part, and the modeling error and gain mismatch are compensated by the data-driven approach via constructing a parameterized finite impulse response filter. In order to diminish the effect of noise, an instrumental variable method is adopted in the cost criterion. The proposed controller has an analytic solution and retains stability during iterations, which is verified on a piezo nanopositioner. Comparative experimental results indicate that the proposed controller can realize flexible tracking in comparison with norm optimal ILC, and achieve the best performance compared with zero-phase-error tracking controller and polynomial basis functions feedforward controller.

## Keywords

Feedforward control, iterative learning control, model-data integrated method, flexible tracking, nanopositioner

## Introduction

Precise motion tracking plays an important role in many modern industrial equipment and scientific instruments, especially at microscale and below. Hence, precise motion control is essential for applications such as wafer stages (Lan et al., 2007), atomic force microscopes (AFMs) (Binnig et al., 1986), information storage (Eleftheriou et al., 2003) and so on. In general, feedback-only design cannot achieve the best performance for the practical and fundamental algebraic restrictions (Lee and Salapaka, 2008). The combination of feedback and feedforward controllers is a promising control scheme, where the feedback controller is designed to retain stability and attenuate unknown disturbances and noise, and the feedforward controller can compensate the tracking errors and known disturbances. Therefore, the design of a feedforward controller is a key component for significant performance enhancement.

Iterative learning control (ILC) is a popular feedforward controller for repetitive reference tracking. The tracking errors are compensated by learning from the previous iterations and updating the control signal for the next iteration (Bristow et al., 2006; Freeman et al., 2010; Wang et al., 2013). The convergence property and robustness to uncertainties and disturbances have been widely studied in Norrlof and Gunnarsson (2010), Ahn et al. (2007) and Norrlof (2004). However, a key assumption for traditional ILC is that the reference signal

should be strictly repetitive (Bristow et al., 2006), and the change of reference during iterations will deteriorate tracking performance significantly, and even result in system divergence (Meulen et al., 2008). In this regard, traditional ILC has lower ability for flexible tracking.

In order to minimize tracking errors and maintain tracking flexibility simultaneously, different tasks were constructed by the repeated basic tasks trained via ILC and the optimal control signal was obtained by fitting the relevant basic tasks or primitives to realize flexible tracking in Hoelzle et al. (2011) and Radac et al. (2015). It should be noted that the tracking references are limited by the numbers of the basic tasks or primitives. Although providing flexible tracking to some extent, these methods cannot track arbitrary references.

To improve tracking flexibility further, model-based feedforward controllers provide good performance via approximate inversion of plant, such as high-order feedforward (Lambrechts, 2005). However, for systems with non-collocated actuators and sensors, such as nanopositioner,

The School of Power and Mechanical Engineering at Wuhan University,  
P.R. China

## Corresponding author:

Xiaohui Xiao, The School of Power and Mechanical Engineering at  
Wuhan University, Wuhan, Hubei Province, P.R. China.

Email: xhxiao@whu.edu.cn

where non-minimum phase (NMP) zeros always exist (Clayton et al., 2009), direct inversion results in unstable feedforward controllers. To overcome this problem, some approximate inversion methods have been proposed. These include zero-phase-error tracking controller (ZPETC) (Tomizuka, 1987), zero-magnitude-error tracking controller (ZMETC) (Butterworth et al., 2012) and non-minimum-phase zeros ignore controller (Fujimoto et al., 2001). The performance of model-based feedforward controllers hinges on the accuracy of the identified model. However, the variation of plant is inevitable during executing tasks for complex systems and modeling error will deteriorate the performance severely for precise tracking.

The modeling errors can be eliminated by data-driven methods (Heertjes and Van Engelen, 2011; Janssens et al., 2013; Kim and Zou, 2013). The control input or parameters can be obtained via calculating the collected data without the knowledge of the plant. In Kim and Zou (2013) and Janssens et al. (2013), the control signals were updated by estimating the impulse response and nonparametric model in frequency domain respectively. However, those methods are still sensitive to reference variation. The polynomial basis functions were employed as the feedforward controller by constructing the finite impulse response (FIR) filter for flexible tracking (De Wijveven and Bosgra, 2010; Meulen et al., 2008). Although the FIR filter is always stable and exists analytic solution, it can only approximate the system with finite poles that is rare in practice for complex dynamic system. On the other hand, rational basis functions parameterized as an infinite impulse response (IIR) filter were also proposed to approximate the plant inversion containing both poles and zeros via ILC (Bolder and Oomen, 2015; Van Zundert et al., 2016). Despite that the method can capture the dynamics effectively, the solution is nonanalytic because the structure of IIR filter is non-convex for optimization. Moreover, the extra tedious iterations should be processed to obtain the parameters and the stability cannot be guaranteed.

Hence, it can be concluded that traditional ILC is sensitive to reference variation, model-based feedforward controllers have low tolerance on modeling error and the implementation of ILC with rational basis functions is complex. To tackle above drawbacks, a model-data integrated ILC for flexible tracking is proposed in this paper. The poles and stable zeros are made use of to compose the model-based part and the modeling error as well as gain mismatch are compensated by data-driven approach via constructing a parameterized FIR filter to make an analytic solution. Besides, similar to Boeren et al. (2015, 2016), an instrumental variable (IV) method is utilized for unbiased estimation to obtain the optimal parameters and diminish the effect of noise. The proposed method can track varying references and maintain precise tracking performance simultaneously with the merits of simplification and practicability for application.

The rest of paper is organized as follows. In ‘Problem formulation’, the problem for flexible tracking is stated. The design of the proposed controller is described in ‘Model-data integrated iterative learning control’. Experiments on a piezo nanopositioner and comparisons of the results are elaborated in ‘Application to a piezo nanopositioner’ and the ‘Conclusion’ completes the paper.

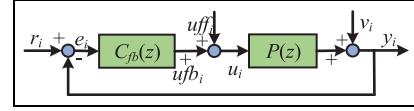


Figure 1. Block diagram of the feedback-feedforward control scheme.

## Problem formulation

### System description

A single-input-single-output (SISO), discrete-time and linear time-invariant system is considered in this paper. The control scheme is shown in Figure 1.  $P(z)$  and  $C_{ff}(z)$  with forward time-shift operator  $z$  indicate the plant and feedback controller.  $y_i$  is the plant output when the input reference is  $r_i$  during the  $i^{\text{th}}$  iteration. The control force  $u_i$  is determined by the sum of the feedforward control signal  $u_{ff_i}$  and feedback control signal  $u_{fb_i}$  together.  $e_i$  is the tracking error and  $v_i$  is the unknown noise.

Considering the signal sequences with length  $N$ , the system can also be presented in lifted domain (Bristow et al., 2006). Take  $P(z)$  with a relative degree  $m$ , for example.  $u_i(k)$  is the input at the time  $k \in \{0, 1, \dots, N-1\}$  and  $y_i(k)$  is the output at the time  $k \in \{m, m+1, \dots, N+m-1\}$ , then the dynamics of  $P(z)$  is equivalent to a  $N \times N$  dimensional lifted matrix with

$$\underbrace{\begin{bmatrix} y_i(m) \\ y_i(m+1) \\ \vdots \\ y_i(N+m-1) \end{bmatrix}}_{y_i} = \underbrace{\begin{bmatrix} h(m) & 0 & \dots & 0 \\ h(m+1) & h(m) & \dots & 0 \\ \vdots & \vdots & \ddots & \vdots \\ h(N+m-1) & h(N+m-2) & \dots & h(m) \end{bmatrix}}_P \underbrace{\begin{bmatrix} u_i(0) \\ u_i(1) \\ \vdots \\ u_i(N-1) \end{bmatrix}}_{u_i} + \underbrace{\begin{bmatrix} v_i(0) \\ v_i(1) \\ \vdots \\ v_i(N-1) \end{bmatrix}}_{v_i} \quad (1)$$

where  $h(k)$ ,  $k \in \{m, m+1, \dots, N+m-1\}$  is the impulse response of  $P(z)$ , given by

$$P(z) \approx h(m) + h(m+1)z^{-1} + h(m+2)z^{-2} + \dots + h(N+m-1)z^{-(N-1)} \quad (2)$$

and other lifted matrices expressed in bold in this paper are calculated similarly as  $P(z)$ .

According to Figure 1, the output and tracking error of the plant are obtained as

$$y_i = \mathbf{T}r_i + \mathbf{S}Puff_i + \mathbf{S}v_i \quad (3)$$

$$e_i = \mathbf{S}r_i - \mathbf{S}Puff_i - \mathbf{S}v_i \quad (4)$$

where  $\mathbf{S}, \mathbf{T}$  and  $\mathbf{S}P$  are the lifted matrices of sensitive transfer function  $S(z) = (1 + P(z)C_{ff}(z))^{-1}$ , complementary sensitivity transfer function  $T(z) = 1 - S(z)$  and process sensitive transfer function  $S(z)P(z)$ , respectively. Hence, for repetitive reference, the error in  $i+1$  iteration is denoted as

$$e_{i+1} = \mathbf{S}r_{i+1} - \mathbf{S}Puff_{i+1} - \mathbf{S}v_{i+1} \quad (5)$$

Under the assumption that the noise is equal to zero and  $r_{i+1} = r_i$ , the error propagation from the  $i^{\text{th}}$  to  $i + 1^{\text{th}}$  iteration can be expressed as

$$e_{i+1} = e_i - SP(uff_{i+1} - uff_i) \tag{6}$$

### Norm optimal iterative learning control

Norm optimal iterative learning control (NOILC) is a popular feedforward controller via minimizing the quadratic criterion of the tracking error and control signal (Gunnarsson and Norrlof, 2001). The optimal control force is calculated by the following cost criterion.

**Definition 1:** The cost criterion for NOILC algorithm is described as

$$J_1 = \|e_{i+1}\|_{W_e}^2 + \|uff_{i+1}\|_{W_u}^2 + \|uff_{i+1} - uff_i\|_{W_{du}}^2 \tag{7}$$

where  $\|x\|_W^2 = W^T x W$ ,  $x \in R^N$ ,  $W_e$  is a  $N \times N$  positive-definite matrix and  $W_u, W_{du}$  are  $N \times N$  positive-semidefinite matrices. The optimal control signal  $uff^*$  is obtained by

$$uff^* = \arg \min_{uff \in R^N} J_1 \tag{8}$$

The solution of equation (8) is given by Theorem 1.

**Theorem 1:** The analytic solution of NOILC that meets equation (8) is described as

$$\begin{cases} uff_{i+1}^* = Q_{NO}uff_i + L_{NO}e_i, \text{ with} \\ Q_{NO} = ((SP)^T W_e (SP) + W_u + W_{du})^{-1} ((SP)^T W_e (SP) + W_{du}) \\ L_{NO} = ((SP)^T W_e (SP) + W_u + W_{du})^{-1} (SP)^T W_e \end{cases} \tag{9}$$

**Proof:** Substitute equation (6) to  $\left(\frac{\partial J_1}{\partial uff_{i+1}}\right)^T$ , and it can be deduced as

$$\left(\frac{\partial J_1}{\partial uff_{i+1}}\right)^T = 2(SP)^T W_e (SP)uff_{i+1} + 2W_uuff_{i+1} + 2W_{du}uff_{i+1} - 2(SP)^T W_e e_i - 2(SP)^T W_e (SP)uff_i - 2W_{du}uff_i \tag{10}$$

Setting equation (10) to zero and rearranging the solution, Theorem 1 is obtained.

NOILC can achieve excellent performance when the reference is strictly repetitive. For  $W_e > 0$  and  $W_u = 0, W_{du} = 0$ , the steady state control force can be found as

$$uff^* = P^{-1}r_j \tag{11}$$

Hence, according to equation (6), the error of next iteration is demonstrated as

$$e_{i+1} = Sr_{i+1} - SPuff^* = Sr_{i+1} - Sr_i \tag{12}$$

From equation (12), it can be concluded that if the reference is repetitive, the convergence error is zero, and if  $r_{i+1} \neq r_i$ , the tracking performance will be deteriorated significantly. That is to say that the traditional ILC cannot handle flexible

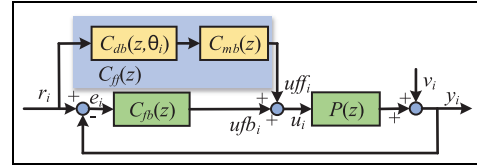


**Figure 2.** Control scheme of the proposed controller.

tracking perfectly. Besides, the design of NOILC relies on the accurate model to obtain  $SP$ . Although in Janssens et al. (2013), a data-driven NOILC was proposed without modeling process, an extra impulse response experiment should be processed firstly and the estimation of impulse response is biased.

### Control objective

In brief, for flexible tracking with excellent performance, a model-data integrated ILC is proposed in this paper to alleviate the assumption that the references to track should be same in traditional ILC. The control object is listed as follows:

- (1) The feedforward controller has the ability to track varying references.
- (2) The optimization of the cost criterion has an analytic solution.
- (3) The trial for experiments is minimum and the controller is stable during iterative process.
- (4) The estimation of parameters is unbiased, despite that noise exists.

## Model-data integrated iterative learning control

### Feedforward controller parameterization

Similar to model-based feedforward controllers, the control force  $uff_i$  should be connected to references  $r_i$  directly to handle the variation of references. The control scheme of model-data integrated ILC is illustrated in Figure 2. Hence, the control force of the feedforward controller is obtained by

$$uff_i = C_{ff}(z)r_i \tag{13}$$

According to equation (5), the error at iteration  $i + 1$  is calculated by substituting to equation (13),

$$e_{i+1} = S(z)(1 - P(z)C_{ff}(z))r_{i+1} - S(z)v_{i+1} \tag{14}$$

if the noise is neglected, the error of each iteration will be zero with  $C_{ff}(z) = P(z)^{-1}$ , that is, the inversion of  $P(z)$ . Therefore, the object (1) is achieved under the control scheme.

For general model-based controllers, the control performance is determined by the accuracy of the identified model  $P(z)$ , which is difficult to obtain in practice for complex dynamics. Hence, the feedforward controller in this paper is parameterized as a model-data integrated feedforward controller. The identified poles and stable zeros compose the

model-based part and the modeling error as well as gain mismatch is compensated by data-based approach.

Considering the plant  $P(z)$  with NMP zeros, it can be decomposed into the stable part and unstable part as ZPETC,

$$P(z) = \frac{B_s(z)B_u(z)}{A(z)} \quad (15)$$

where  $A(z)$  contains the identified poles, and  $B_s(z), B_u(z)$  are composed by stable zeros and unstable zeros respectively. The model-base part is obtained by inverting the poles and stable zeros in order to stabilize the controller. Therefore, the model-based part  $C_{mb}(z)$  in Figure 2 is expressed as

$$C_{mb}(z) = \frac{A(z)}{z^d B_s(z)} \quad (16)$$

where  $d$  is the difference between poles and stable zeros to make  $C_{mb}(z)$  causal. Being different from the design of ZPETC, a data-based FIR filter is adopted to compensate the NMP zeros caused inversion error and model uncertainties through iteration. The structure of data-based part is expressed in Definition 2.

**Definition 2:** The feedforward controller of the data-based part  $C_{db}(z, \theta_i)$  parameterized as a FIR filter structure is defined as

$$C_{db}(z, \theta_i) = \sum_{j=1}^n \theta_j [j] z^{-j} \quad (17)$$

here,  $\theta_i \in \mathbf{R}^n$  is the parametric vector of the FIR filter coefficients. In lifted domain, equation (17) can also written as

$$C_{db}(\theta_i) = \sum_{j=1}^n \psi_j \theta_i [j] \quad (18)$$

where  $\psi_j$  is the lifted matrix of  $z^{-j}$ , which indicates the  $j$ -step time delay for the input signal.

Therefore, according to Figure 2, the model-data integrated feedforward controller  $C_{ff}(z, \theta_i)$  and feedforward control force  $uff_i$  are parameterized as

$$C_{ff}(z, \theta_i) = C_{db}(z, \theta_i) C_{mb}(z) \quad (19)$$

$$uff_i = C_{ff}(z, \theta_i) r_i \quad (20)$$

The parameters are linear to  $C_{ff}(z, \theta_i)$  from equation (17) and equation (18). Hence, the optimization problem with quadric form is convex. Besides, the stable part of identified model and data-based part with FIR filter structure always guarantee the stability of the proposed controller so that the object (2) and (3) are realized.

### Parameters optimization

To obtain the parameters in equation (18), a data-based method is adopted to optimize the tracking performance. Substituting equation (19) to equation (3), the output in the  $i^{th}$  iteration is given as

$$y_i = \mathbf{SP}(C_{fb} + C_{ff}(\theta_i))r_i + \mathbf{S}v_i \quad (21)$$

Assuming that  $v_i = \mathbf{0}$ , equation (21) can be rewritten as

$$\widehat{\mathbf{SP}}r_i = (C_{fb} + C_{ff}(\theta_i))^{-1}y_i = C(\theta_i)^{-1}y_i \quad (22)$$

where  $\widehat{\mathbf{SP}}$  means the estimation of  $\mathbf{SP}$  with the measured data  $y_i$  and  $C(\theta_i)$  is the lifted matrix of  $C(z) = C_{fb}(z) + C_{ff}(z, \theta_i)$ . Hence, the estimated error of next iteration is obtained by

$$\widehat{e}_{i+1}(\theta_{i+1}) = e_i - (C_{ff}(\theta_{i+1}) - C_{ff}(\theta_i))C(\theta_i)^{-1}y_i \quad (23)$$

Furthermore, the term  $C(\theta_i)^{-1}y_i$  can be deemed as the signal  $y_i$  filtered by  $C(z)^{-1}$ . However,  $C(z)^{-1}$  may be unstable during iterative process. A technology introduced in Kinoshita et al. (2002) is used in this paper that separates the stable and unstable mode of  $C(z)^{-1}$ , as expressed in equation (24)

$$C(z)^{-1} = C(z)_{stable}^{-1} + C(z)_{unstable}^{-1} \quad (24)$$

which can be obtain by *stabsep* command in MATLAB. The stable part  $C(z)_{stable}^{-1}$  is used to filter the forward time of  $y_i$ , and the unstable part  $C(z)_{unstable}^{-1}$  is used to filter the negative time of  $y_i$ , which can be calculated off-line after each iteration. In the following section, the signal  $y_i$  filtered by  $C(z)^{-1}$  is calculated by the above method.

It should be noted that equation (23) only contains the measured signals without the plant information. However, the noise always exists in the closed-loop system, such as the quantization noise of sensors, which will result in a biased estimation of  $\theta_i$  (Boeren et al., 2015). Hence, an instrumental variable (IV) method (Ljung, 1999) is utilized for an unbiased estimation. The cost criterion with IV is defined as follows.

**Definition 3:** The cost criterion to obtain optimal parametric vector is given as

$$J_2(\theta_{i+1}) = \|\mathbf{W}^T \widehat{e}_{i+1}(\theta_{i+1})\|_{\mathbf{W}_e}^2 + \|\mathbf{uff}_{i+1}(\theta_{i+1})\|_{\mathbf{W}_u}^2 + \|\mathbf{uff}_{i+1}(\theta_{i+1}) - \mathbf{uff}_i\|_{\mathbf{W}_{du}}^2 \quad (25)$$

where  $\mathbf{W} \in \mathbf{R}^{N \times n}$  is the IV.

The selection of  $\mathbf{W}$  is important to estimate the optimal parameters. In general,  $\mathbf{W}$  should be uncorrelated with noise  $v_i$ , and correlated with  $u_i$  and  $y_i$ . Hence, in this paper,  $\mathbf{W}$  is chosen as,

$$\mathbf{W} = [\psi_1 r_i, \psi_2 r_i, \dots, \psi_j r_i] \quad (26)$$

And the object (4) is achieved via equation (26).

### Model-data integrated control law

The control law is calculated by minimizing the cost criterion  $J_2(\theta_{i+1})$  to get

$$\theta^* := \arg \min_{\theta \in \mathbf{R}^n} J_2(\theta_{i+1}) \quad (27)$$

The analytic solution of equation (27) is given by Theorem 2.

**Theorem 2:** The control law of model-data integrated ILC is demonstrated as

$$\begin{cases} \theta_{i+1} = Q_{MDI} \theta_i + L_{MDI} e_i, \text{ with} \\ \mathbf{H} = (W^T C_{mb} \psi_{C(z)^{-1}, y_i})^T W^T W_e C_{mb} \psi_{C(z)^{-1}, y_i} \\ \quad + (C_{mb} \psi_{r_i})^T W_u (C_{mb} \psi_{r_i}) + (C_{mb} \psi_{r_i})^T W_{du} (C_{mb} \psi_{r_i}) \\ Q_{MDI} = \mathbf{H} \setminus ((W^T C_{mb} \psi_{C(z)^{-1}, y_i})^T W^T W_e C_{mb} \psi_{C(z)^{-1}, y_i} \\ \quad + (C_{mb} \psi_{r_i})^T W_{du} (C_{mb} \psi_{r_i})) \\ L_{MDI} = \mathbf{H} \setminus ((W^T C_{mb} \psi_{C(z)^{-1}, y_i})^T W^T W_e) \end{cases} \quad (28)$$

where  $C(z) = C_{fb}(z) + C_{ff}(z, \theta_i)$ ,  $\psi_{C(z)^{-1}, y_i} = [\psi_1 C(z)^{-1} y_i, C(z)^{-1} y_i, \dots, \psi_j C(z)^{-1} y_i]$ , and  $\psi_{r_i} = [\psi_1 r_i, \psi_2 r_i, \dots, \psi_j r_i]$ .

**Proof:** Substitute equation (23) to Definition 2, and use the following equation

$$\frac{\partial(\|Ax + b\|_Q^2)}{\partial x} = 2(Ax + b)^T QA \quad (29)$$

where  $x, b \in R^n, A \in R^{N \times N}$  and  $Q = Q^T \in R^{N \times N}$ . By expressing as lifted matrices and differentiating  $J_2(\theta_{i+1})$  with respect to  $\theta_{i+1}$ , it is obtained that

$$\begin{aligned} \frac{1}{2} \left( \frac{\partial J_2(\theta_{i+1})}{\partial \theta_{i+1}} \right)^T &= -(W^T C_{mb} \psi_{C(z)^{-1}, y_i})^T W^T \\ &\quad W_e (e_i - C_{mb} \psi_{C(z)^{-1}, y_i} (\theta_{i+1} - \theta_i)) \\ &\quad + (C_{mb} \psi_{r_i})^T W_u (C_{mb} \psi_{r_i}) \theta_{i+1} + (C_{mb} \psi_{r_i})^T \\ &\quad W_{du} (C_{mb} \psi_{r_i}) (\theta_{i+1} - \theta_i) \end{aligned} \quad (30)$$

Setting the above equation to zero and rearranging the terms  $\theta_{i+1}, \theta_i$  and  $e_i$ , Theorem 2 is obtained in lifted domain.

Therefore, the closed-loop transfer function from  $r_{i+1}$  to  $y_{i+1}$  can be expressed as

$$G_{cl}(z) = \frac{P(z)(C_{ff}(z, \theta_{i+1}) + C_{fb}(z))}{1 + P(z)C_{fb}(z)} \quad (31)$$

It should be noted that the stability of  $G_{cl}(z)$  is guaranteed if all poles of  $1 + P(z)C_{fb}(z)$  lie in the unit circle because equation (30) results in the convergence of  $\theta_{i+1}$  and a stable  $C_{ff}(z, \theta_{i+1})$ .

Combining the above results, the following design procedure is proposed for flexible tracking, which represents the main contributions of this paper.

**Procedure 1:** The feedforward controller  $C_{ff}(z, \theta_{i+1})$  is obtained by the following steps:

- (1) By identifying the plant,  $C_{mb}(z)$  is obtained according to equations (15) and (16). Set the initial value of  $\theta_0$  to zero.
- (2) Collect the measured signals  $e_i$  and  $y_i$ .
- (3) Calculate  $\psi_{C(z)^{-1}, y_i} = [\psi_1 C(z)^{-1} y_i, C(z)^{-1} y_i, \dots, \psi_j C(z)^{-1} y_i]$  and construct instrumental variable  $W$  by equation (26).
- (4) Calculate  $\theta_{i+1}$  based on Theorem 2.
- (5) Construct the feedforward controller

$$C_{ff}(z, \theta_{i+1}) = \left( \sum_{j=1}^n \theta_{i+1} [j] z^{-j} \right) C_{mb}(z).$$

- (6) Set  $i$  to  $i + 1$ , and repeat step (2) to step (5).

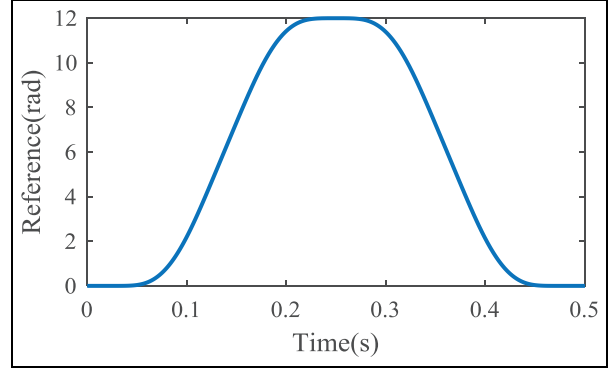


**Figure 3.** Nominal fourth-order reference trajectory.

### Simulation case

To verify the proposed controller preliminarily, a two-mass spring motion system in Boeren et al. (2015) is used for simulation. A fourth-order reference trajectory (Lambrechts, 2005) is adopted and the nominal reference is plotted in Figure 3. Ten difference references were performed with the parameters:  $r_{max} = 12 \sim 14 rad$ ,  $v_{max} = 9000 \sim 10000 rads^{-1}$ ,  $a_{max} = 9000 \sim 10010 rads^{-2}$ ,  $j_{max} = 23 \sim 25 rads^{-3}$ , which were generated randomly and the reference changed after each iteration. The sample rate is 1000Hz and the noise with standard deviation of  $0.002 rad$  was injected into the simulation model.

In order to evaluate the performance of the proposed controller, the following four feedforward controllers were used for comparison:

- (1)  $C_1$ : model-based feedforward controller ZPETC (Tomizuka, 1987).
- (2)  $C_2$ : NOILC (Bristow et al., 2006) in Theorem 1.
- (3)  $C_3$ : polynomial basis functions feedforward controller in Boeren et al. (2015).
- (4)  $C_4$ : model-data integrated ILC proposed in this paper.

Figure 4 shows the results of the Root-Mean-Square (RMS) errors and maximal (MAX) errors of 10 iterations with  $n=4$ . For  $C_1, C_3$  and  $C_4$ , the iterative curves are smooth from  $i=2$  to  $i=10$ , whereas the curves with  $C_2$  shake fiercely because traditional ILC could not handle the varying references. Although  $C_1$  is not sensitive to the change of reference, the performance is still limited by the NMP zeros of the plant which results in an approximate inversion. According to Figure 5, the performance of  $C_4$  is superior to  $C_3$  because the structure of  $C_4$  is an IIR filter that contains both zeroes and poles to capture the resonance peak at 29.3 Hz and anti-resonance peak at 16.3 Hz. However,  $C_3$  can only approximate the lower frequency range, which deteriorates the performance.

## Application to a piezo nanopositioner

### Experimental setup

A three-axis piezo nanopositioner (P-561.3CD, Physik Instrumente) was used for experiments. To perform the four

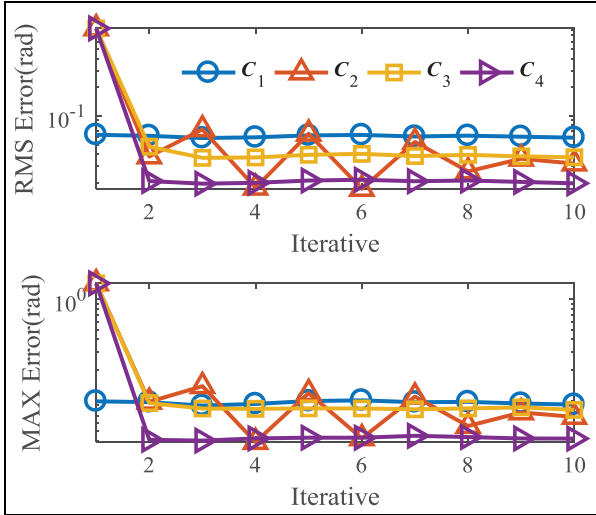


Figure 4. RMS and MAX errors in simulations.

controllers, only the  $x$  axis with a stroke of  $100\mu\text{m}$  was experimented for comparison. The control input voltage (0–10 V) is produced by 16-bit digital to analog converters (DACs) of the data acquisition card (PCI 6289, National Instrument) for the piezo amplifier module with a fixed gain 10 (E-503.00, Physik Instrumente) and the sensor data is collected by the data acquisition card (PCI 6289, National Instrument) equipped with 18-bit analog to digital converters (ADCs) through sensor monitor (E-509.C3A, Physik Instrumente). The controllers were designed in Matlab/Simulink on develop PC and implemented on the target PC in real-time after compiling. The sampling frequency of the system is set to 10 kHz. Figure 6 shows the experimental setup.

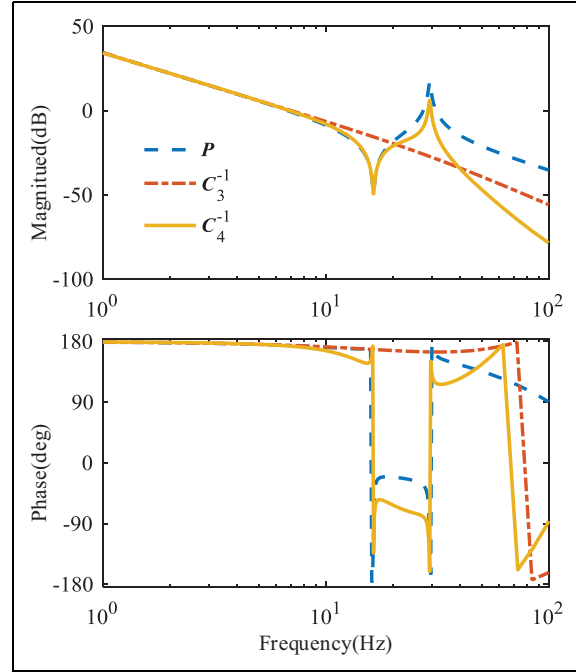


Figure 5. Bode diagram of nominal model and inversion of  $C_3, C_4$  at the 10<sup>th</sup> iteration in simulations.

In order to identify the system, a set of 100mV swept sine waves between 0.1Hz and 500Hz were applied to the  $x$  axis. It should be noted that a low amplitude signal was used in order to minimize the hysteresis nonlinearity. A continuous transfer function was obtained by *invfreqs* command in MATLAB, and discretized via zero-order holder (ZOH) method. The transfer function of  $P(z)$  is given by

$$P(z) = \frac{0.011003(z - 0.9967)(z^2 - 2z + 0.9996)(z^2 - 1.7z + 0.9532)(z^2 - 2.03z + 5.045)}{(z - 0.796)(z - 0.9969)(z^2 - 2z + 0.9995)(z^2 - 1.418z + 0.6218)(z^2 - 1.544z + 0.9635)} \quad (32)$$

Figure 7 shows the match between the measured and identified open-loop frequency response. Besides, it is clear that a

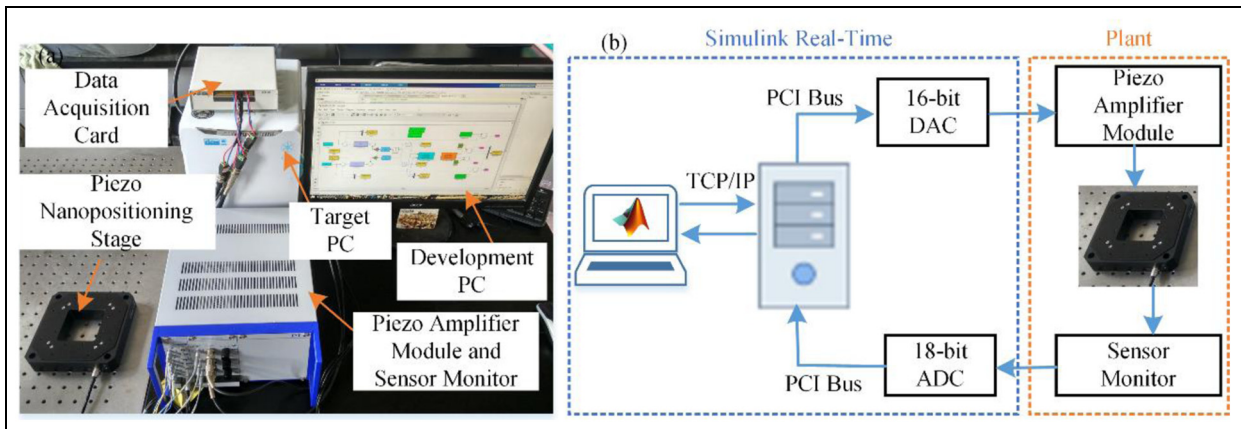
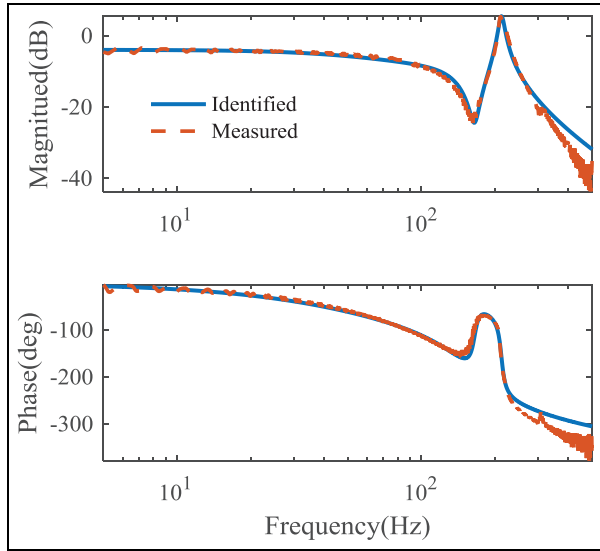
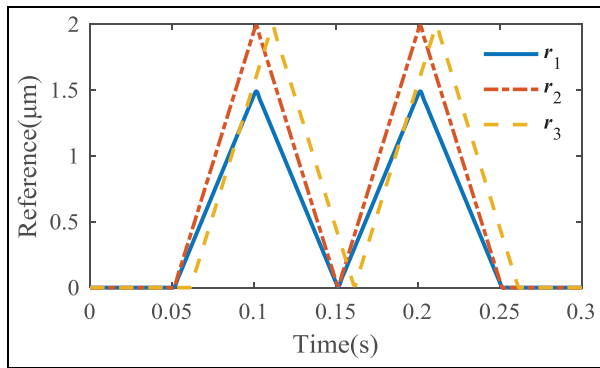


Figure 6. The experimental setup of nanopositioner (a) Experimental platform (b) Block diagram.



**Figure 7.** The measured and the identified model amplitude frequency responses.



**Figure 8.** Varying references for experiments.

**Table 1.** Statistical results of fixed reference tracking at the 8<sup>th</sup> iteration.

Controller	RMS Errors(nm)	MAX Errors(nm)
$C_1$	49.65	138.70
$C_2$	5.88	28.45
$C_3$	30.80	99.03
$C_4$	16.01	62.17

pair of NMP zeros exists according to equation (32), which is common in nanopositioning system. Therefore, the model-based part of the proposed controller was obtained by the poles and stable zeros in equation (32), given by

$$C_{mb}(z) = \frac{(z - 0.796)(z - 0.9969)(z^2 - 2z + 0.9995)(z^2 - 1.418z + 0.6218)(z^2 - 1.544z + 0.9635)}{z^3(z - 0.9967)(z^2 - 2z + 0.9996)(z^2 - 1.7z + 0.9532)} \quad (33)$$

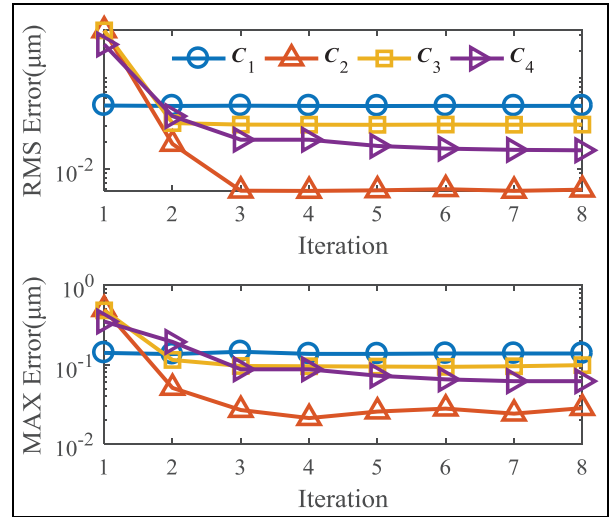


**Figure 9.** RMS and MAX errors of fixed reference tracking.

To deal with the low-gain margin of nanopositioning system, a notch filter to suppress the effect of the dominant resonant peak was implemented for the cascade of a high-gain proportion-integration (PI) controller that can be used to account for hysteresis and creep nonlinearity. Three references defined for experiments are shown in Figure 8.  $r_1$  is a 10 Hz triangular wave with the peak-to-peak amplitude of  $1.5\mu\text{m}$ . The amplitude of  $r_2$  expand 1/3 times relative to  $r_1$ , that is,  $2\mu\text{m}$  and  $r_3$  is equal to  $r_2$  with 0.01s delay. The amplitude is small so that the system behavior is approximately linear.

### Results of tracking fixed reference

Eight iterations were performed for fixed reference tracking with reference  $r_2$ . For  $C_3$  and  $C_4$ , the order of FIR filters were chosen as  $n=4$ , and the initial value of  $\theta_0$  was set to zero so that the results of the first iteration is with feedback controller only.

The RMS and MAX errors versus iteration are shown in Figure 9. The tracking performance with feedback controller only was the worst with the RMS error of  $0.3386\mu\text{m}$  and MAX error of  $0.4844\mu\text{m}$  for the phase delay and no ability to compensate repetitive errors. The errors of the last iteration were plotted in Figure 10 and the statistical results at 8<sup>th</sup> iteration were listed in Table 1. For feedforward controllers, the errors of  $C_1$  were the largest because it was designed by model-based method and there were no parameters changing during iterations so that the modeling error cannot be compensated.  $C_2$  achieved the best performance with RMS error of 5.88nm and MAX error of 25.48nm respectively. It should be noted that compared to  $C_3$  with  $n=4$ , for repetitive reference tracking,  $C_2$  can be viewed as the FIR filter with  $n=N$ .

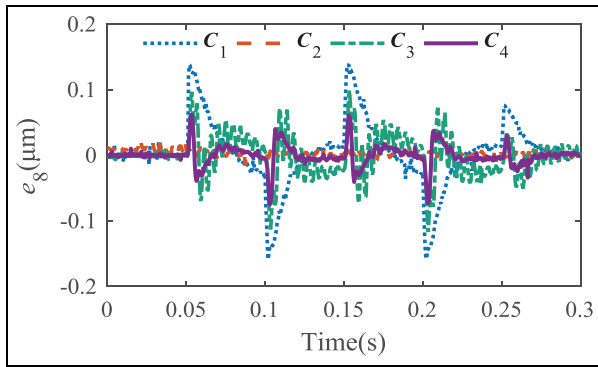


Figure 10. Tracking errors of fixed reference at the 8<sup>th</sup> iteration.

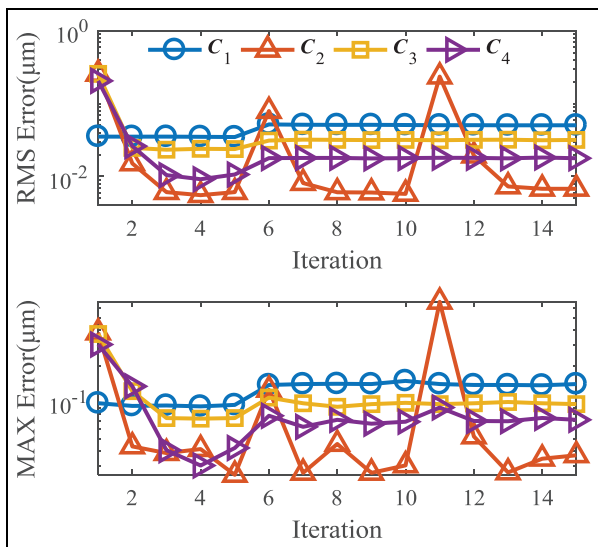


Figure 11. RMS and MAX errors of varying references tracking.

For the proposed controller  $C_4$ , the RMS error was 16.01nm and the MAX error was 62.17nm, which outperform the performance of  $C_3$  for the structure of IIR filter that can approximate the dynamics more accurately than FIR filter. However,  $C_2$  can achieve the best performance with fixed reference tracking for the characteristic of improving the system

bandwidth, which can be concluded from Figure 10, where the errors of  $C_2$  are minimum although at the corner of triangular wave.

Results of tracking varying references

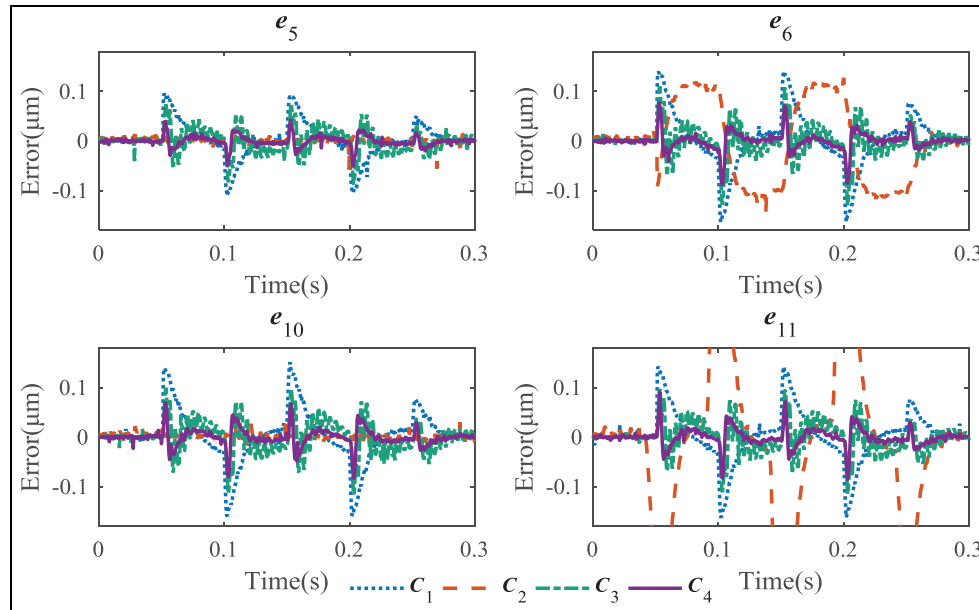
To demonstrate the ability of flexible tracking of the proposed controller, 15 iterations were conducted in experiments with four different controllers. The references were shown in Figure 8, where the input signals were  $r_1$ ,  $r_2$  and  $r_3$  between the 1<sup>st</sup> iteration and 5<sup>th</sup> iteration, 6<sup>th</sup> iteration and 10<sup>th</sup> iteration, 11<sup>th</sup> iteration and 15<sup>th</sup> iteration, respectively. Similar to fixed reference tracking, the order of FIR filter was chosen as  $n=4$  for  $C_3$  and  $C_4$ , and the initial value of  $\theta_0$  was set to zero.

The tracking results were demonstrated in Figure 11 and Figure 12. The statistical results were listed in Table 2. It is clear that the four controllers improve the performance significantly compared with feedback controller only at the 1<sup>st</sup> iteration.  $C_2$  is sensitive to the change of references, which can be concluded in Figure 11, where the RMS errors change from 6.01nm to 78.93nm at the 5 iteration and 6<sup>th</sup> iteration, from 5.77nm to 234.20nm at the 10<sup>th</sup> iteration and 11<sup>th</sup> iteration because the control signal of tradition ILC determined by errors of previous iterations only have no connection with references.  $C_1$ ,  $C_3$  and  $C_4$  have the ability to handle varying references according to Figure 11 and Figure 12. Note that the errors between the 6<sup>th</sup> iteration and 10<sup>th</sup> iteration increase lightly for the reference amplitude changing from 1.5 $\mu$ m to 2 $\mu$ m. The performance of  $C_1$  is deteriorated by the NMP zeros in the plant and model uncertainties during iterations. For  $C_3$  and  $C_4$ , taking the 5<sup>th</sup> iteration as example,  $C_4$  achieved the performance with RMS errors of 10.64nm and MAX errors of 42.23nm compared with 23.75nm and 74.23nm for  $C_3$  respectively. The proposed model-data integrated IIR filter structure outperform the FIR filter structure and can achieve precision flexible tracking simultaneously.

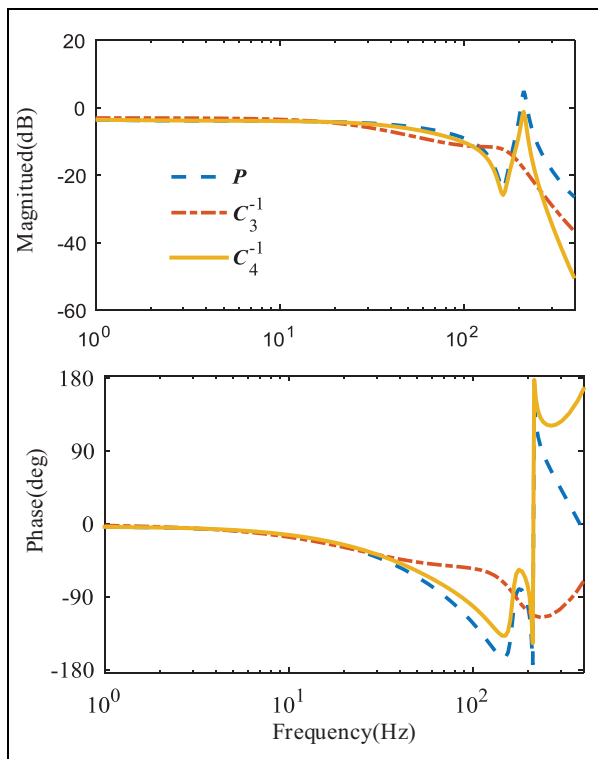
In the perspective of frequency domain, Figure 13 showed the bode diagram of the nominal model and the inversion of  $C_3$  and  $C_4$  at the 15<sup>th</sup> iteration. It demonstrates that  $C_4$  can capture the resonance peak at 212 Hz and the anti-resonance peak at 160 Hz for the contained zeros and poles, whereas  $C_3$  can only approximate the lower frequency that deteriorates the performance.

Table 2. Statistical results for varying references.

Controller	RMS Errors(nm)				MAX Errors(nm)			
	$e_5$	$e_6$	$e_{10}$	$e_{11}$	$e_5$	$e_6$	$e_{10}$	$e_{11}$
$C_1$	34.70	51.72	50.76	50.46	95.67	139.70	150.90	142.10
$C_2$	6.01	78.93	5.77	234.20	25.35	137.40	30.34	677.90
$C_3$	23.75	31.05	31.71	31.37	74.50	109.90	99.50	91.03
$C_4$	10.64	17.84	17.85	18.01	42.23	77.86	69.52	70.50



**Figure 12.** Track errors at the 5<sup>th</sup>, 6<sup>th</sup>, 10<sup>th</sup> and 11<sup>th</sup> iteration respectively.



**Figure 13.** Bode diagram of nominal model and inversion of  $C_3$ ,  $C_4$  at the 15<sup>th</sup> iteration in experiments.

### Conclusion

In this paper, a model-data integrated ILC was developed to track varying references for precise motion systems with complex and NMP dynamics. Compared with pure model-based

feedforward and data-based controller, the proposed method takes full advantage of the information of identified model to compose model-based part and the collected data to get optimal parameters of the data-based FIR filter. The effect of noise was reduced through implementing IV method and the feedforward controller is stable during iterations. The performance was verified through simulation, which shows that the proposed controller can handle the problem of flexible tracking effectively. The controller was also implemented on a piezo nanopositioner. The experimental results demonstrate that NOILC achieved the best performance for fixed reference, whereas the tracking errors increase when the reference changing. For varying references tracking, the performance of proposed controller outperforms ZPETC for the compensation of modeling error via collected data and polynomial basis functions feedforward controller for the structure of IIR filter that can approximate the inverse plant dynamics accurately. The future work will concentrate upon the improvement of tracking bandwidth, such as minimizing errors at the corner of triangular wave and realizing flexible tracking on multiple-input-multiple-output (MIMO) systems.

### Declaration of conflicting interest

The authors declare that there is no conflict of interest.

### Funding

This work was supported by the Natural Science Foundation of China under Grant 51375349.

### References

Ahn H, Chen Y and Moore KL (2007) Iterative learning control: Brief survey and categorization. *Systems Man and Cybernetics* 37(6): 1099–1121.

- Binnig G, Quate CF and Gerber C (1986) Atomic force microscope. *Physical review letters* 56(9): 930–933.
- Boeren F, Bruijnen D and Oomen T (2016) Enhancing feedforward controller tuning via instrumental variables: With application to nanopositioning. *International Journal of Control* 90(4): 746–764.
- Boeren F, Oomen T and Steinbuch M (2015) Iterative motion feedforward tuning: A data-driven approach based on instrumental variable identification. *Control Engineering Practice* 37: 11–19.
- Bolder J and Oomen T (2015) Rational basis functions in iterative learning control—With experimental verification on a motion system. *IEEE Transactions on Control Systems and Technology* 23(2): 722–729.
- Bristow DA, Tharayil M and Alleyne A (2006) A survey of iterative learning control. *IEEE Control Systems Magazine* 26(3): 96–114.
- Butterworth JA, Pao LY and Abramovitch DY (2012) Analysis and comparison of three discrete-time feedforward model-inverse control techniques for nonminimum-phase systems. *Mechatronics* 22(5): 577–587.
- Clayton GM, Tien S, Leang KK, et al. (2009) A review of feedforward control approaches in nanopositioning for high-speed SPM. *Journal of Dynamic Systems Measurement and Control-transactions of The Asme* 131(6): 061101.
- De Wijdeven JV and Bosgra OH (2010) Using basis functions in iterative learning control: Analysis and design theory. *International Journal of Control* 83(4): 661–675.
- Eleftheriou E, Antonakopoulos T, Binnig G, et al. (2003) Millipede-a MEMS-based scanning-probe data-storage system. *IEEE Transactions on Magnetics* 39(2): 938–945.
- Freeman C, Lewin P, Rogers E, et al. (2010) Iterative learning control applied to a gantry robot and conveyor system. *Transactions of the Institute of Measurement & Control* 32(3): 251–264.
- Fujimoto H, Hori Y and Kawamura A (2001) Perfect tracking control based on multirate feedforward control with generalized sampling periods. *IEEE Transactions on Industrial Electronics* 48(3): 636–644.
- Gunnarsson S and Norrlof M (2001) Brief On the design of ILC algorithms using optimization. *Automatica*.
- Heertjes MF and Van Engelen A (2011) Minimizing cross-talk in high-precision motion systems using data-based dynamic decoupling. *Control Engineering Practice* 19(12): 1423–1432.
- Hoelzle DJ, Alleyne A and Johnson AJW (2011) Basis task approach to iterative learning control with applications to micro-robotic deposition. *IEEE Transactions on Control Systems and Technology* 19(5): 1138–1148.
- Janssens P, Pipeleers G and Swevers J. (2013) A data-driven constrained norm-optimal iterative learning control framework for LTI Systems. *IEEE Transactions on Control Systems Technology* 21(2): 546–551.
- Kim K and Zou Q (2013) A modeling-free inversion-based iterative feedforward control for precision output tracking of linear time-invariant systems. *IEEE-ASME Transactions on Mechatronics* 18(6): 1767–1777.
- Kinosita K, Sogo T and Adachi N (2002) Iterative learning control using adjoint systems and stable inversion. *Asian Journal of Control* 4(1): 60–67.
- Lambrechts P (2005) Trajectory planning and feedforward design for electromechanical motion systems. *Control Engineering Practice* 13(2): 145–157.
- Lan H, Ding Y, Liu H, et al. (2007) Review of the wafer stage for nanoimprint lithography. *Microelectronic Engineering* 84(4): 684–688.
- Lee C and Salapaka SM (2008) Robust broadband nanopositioning: fundamental trade-offs, analysis, and design in a two-degree-of-freedom control framework. *Nanotechnology* 20(3): 035501.
- Ljung L (1999) System identification: Theory for the user. *Journal of Networks*.
- Meulen SHVD, Tousain RL and Bosgra OH (2008) Fixed structure feedforward controller design exploiting iterative trials: Application to a wafer stage and a desktop printer. *Journal of Dynamic Systems Measurement & Control* 130(5): 556–562.
- Norrlof M (2004) Disturbance rejection using an ILC algorithm with iteration varying filters. *Asian Journal of Control* 6(3): 432–438.
- Norrlof M and Gunnarsson S (2010) Time and frequency domain convergence properties in iterative learning control. *International Journal of Control* 75(14): 1114–1126.
- Radac M, Precup R and Petriu EM (2015) Model-free primitive-based iterative learning control approach to trajectory tracking of MIMO systems with experimental validation. *IEEE Transactions on Neural Networks* 26(11): 2925–2938.
- Tomizuka M (1987) Zero phase error tracking algorithm for digital control. *Journal of Dynamic Systems Measurement and Control-transactions of The Asme* 109(1): 65–68.
- Van Zundert J, Bolder J and Oomen T (2016) Optimality and flexibility in Iterative Learning Control for varying tasks. *Automatica* 67: 295–302.
- Wang S, Wang J and Zhao J (2013) Application of PD-type iterative learning control in hydraulically driven 6-DOF parallel platform. *Transactions of the Institute of Measurement and Control* 35(5): 683–691.